Acta Mech. Sin. (2011) 27(5):687–696
DOI 10.1007/s10409-011-0498-9

RESEARCH PAPER

Interference effects of two and three super-tall buildings under wind action

Ming Gu · Zhuang-Ning Xie

Received: 5 February 2010 / Revised: 24 May 2010 / Accepted: 16 August 2010
©The Chinese Society of Theoretical and Applied Mechanics and Springer-Verlag Berlin Heidelberg 2011

Abstract Most previous investigations on interference effects of tall buildings under wind actions focused on the wind induced interference effects between two buildings, and the interference effects of three or more buildings have seldom been studied so far due to the huge workload involved in experiments and data processing. In this paper, mean and dynamic force/response interference effects and peak wind pressure interference effects of two and three tall buildings, especially the three-building configuration, are investigated through a series of wind tunnel tests on typical tall building models using high frequency force balance technique and wind pressure measurements. Furthermore, the present paper focuses on the effects of parameters, including breadth ratio and height ratio of the buildings and terrain category, on the interference factors and derives relevant regression results for the interference factors.

Keywords Super-tall building · Wind force and response · Interference effect · Wind tunnel test

1 Introduction

Wind loads on tall buildings are usually evaluated based on structural design codes and standards. The specifications for wind loads used in the codes and standards are generally obtained from wind tunnel tests performed on an isolated building. But many studies have shown that, due to the existence of nearby buildings, the wind loads on a building interfered by neighboring buildings may be quite different from those on the same but isolated building.

The existing adjacent buildings may either decrease or increase the wind loads on a building, depending on various geometrical, structural and wind parameters, including size, section shape, relative position of these buildings, reduced wind velocity, number of the adjacent buildings, upstream terrain conditions and so on. The phenomenon, known commonly as the interference effect, is very complicated and must be evaluated properly [1–5].

The wind induced interference has been generally classified into static interference and dynamic interference effects. Previous studies have showed that the interference effects generally induce dynamic load amplification but mean load reduction for the interfered principal building. Bailey and Kwok [6] investigated the enhanced dynamic responses of a tall square building under the interference action from neighboring square and circular buildings. Two-dimensional contour maps were given in their study to describe the variation of the interference factor (IF) versus the position of the interfering building. With these contours, the critical locations for the interfering building and the extent of the interference effect can be easily found. Taniike and Inaoka [7] and Taniike [8,9] investigated the amplified response and the possible aeroelastic mechanism of a tall building under interference excitation of several types of upstream buildings with different breadths in different upstream flow conditions. English [10] suggested a third-order regression polynomial to predict the shielding factors for mean interference effects in the case of a pair of rectangular prisms in tandem. Khanduri et al. [5] and English [11] applied the artificial neural networks (ANN) method to predict the wind induced interference effects. Recently, the authors made wind tunnel tests on two and three tall building models [12–14], especially on three building models [15–17], together with numerical

The project was supported by the National Natural Science Foundation of China (90715040).

M. Gu (✉)
State Key Lab for Disaster Reduction in Civil Engineering,
Tongji University, 200092 Shanghai, China
e-mail: minggu@tongji.edu.cn

Z.-N. Xie
Department of Civil Engineering,
South China University of Technology,
510641 Guangzhou, China

simulations [18,19] to investigate the interference effects of buildings. Moreover, study on wind pressure interference effect is also important for practical purpose but is much more complicated [20]. Besides researches on force/response interference effects as mentioned above, Cheng et al. [21] developed a wind tunnel database including force/response interference factors for the wind resistance design of tall buildings.

This paper summarizes the wind induced interference effects of two and three tall buildings in more detail based on the wind tunnel tests carried out by the authors on tall building models with around 10 000 testing cases using the high frequency force balance technique and wind pressure scan technique. The wind tunnel tests were conducted in STDX-1 Boundary Layer Wind Tunnel in Shantou University and TJ-1 Boundary Layer Wind Tunnel in Tongji University. Some cases of the twin-building configurations were tested in both of the wind tunnels for comparison and complement each other. The emphasis of the paper is laid on the mean and dynamic interference effects and wind pressure interference effects of three tall buildings, especially on the regression results of the mean and dynamic interference factors and wind pressure interference factor.

2 Description of experiment and data processing

2.1 Wind tunnel and wind field simulation

According to the Chinese load code GB50009-2001 [22], the exposure categories B and D, corresponding to exponents of the power law of mean speed profile of 0.16 and 0.30, respectively, were simulated in the wind tunnels at a length scale of 1/400. In order to investigate the effects of terrain conditions on the interference in more detail, the models were also tested in uniform flow.

2.2 Equipment, models and experimental arrangements

As mentioned above, the measurements were carried out using high force balance technique and wind pressure scanning technique. For the force balance test, the principal building model, i.e., the interfered model with a height of 600 mm and a square cross section of breadth of 100 mm, was made of foamed plastics as the core and light wood plates of 1 mm thickness as "clothes" to ensure the model as light as possible, and thus to get the first natural frequencies of the balance-model system as high as possible. The fundamental frequencies of the balance-model systems were all higher than 100 Hz, which are much higher than the concerned frequency range of the aerodynamic forces acting on the building models.

As for the wind pressure measurement wind tunnel test, the principal building model has the same shape as the above-mentioned model. The pressure taps were arranged at the height of 400 mm, i.e. 2/3 height of the building model, as can be seen in Fig. 1. Obviously the wind pressure interference effect is much more complicated than the problems of mean and dynamic interference effects. In Fig. 1, one critical tap point called Point P_1 should be noticed, which is located at the leading edge of the side wall of the building model, just within the flow separation region. Thus, only the interference effects of wind pressure at Point P_1 will be discussed in this paper.

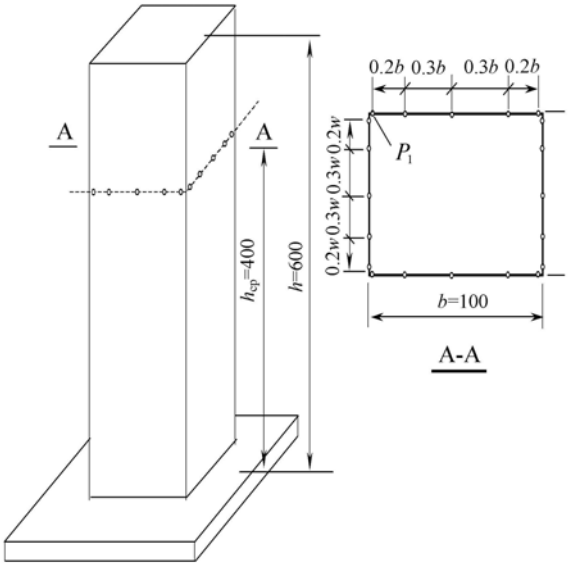

Fig. 1 Principal building model and arrangement of pressure taps

Two groups of interfering models of different heights and cross-section's breadths were adopted in the present test to investigate the interference effects of height and breadth of the upstream building(s) on the principal building. The first group of the interfering buildings have the same height h as the principal building with square cross-section but different breadths of 0.5b, 0.75b, 1.0b, 1.5b and 2.0b, where b (=100 mm) is the breadth of the principal building model; while the second group of interfering models have the same square cross-section as the principal building model but different heights of 0.5h, 0.75h, 1.0h, 1.25h and 1.5h, where h (= 600 mm) is the height of the principal model. The breadth ratio (B_r)/height ratio (H_r) are defined hereafter to be the ratio of the breadth/height of the interfering building(s) to those of the principal building. All the building models are orientated with one face normal to the wind, while the center-to-center spacing among them varies in along-wind direction (x) and across-wind direction (y) in a coordinate grid shown in Fig. 2.

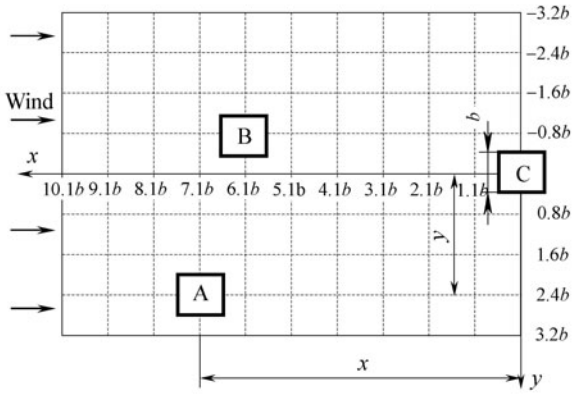

Fig. 2 *X-Y* coordinate grid for positions of interfering buildings

2.3 Testing data processing

The *IF*, which describes quantitatively the interference effects, is defined in the paper as

$$IF = \frac{\begin{array}{l}\text{Wind force (or wind pressure}\\ \text{or dynamic response) of principal}\\ \text{building under interference}\end{array}}{\begin{array}{l}\text{Wind force (or wind pressure}\\ \text{or dynamic response) of isolated}\\ \text{principal building}\end{array}}, \quad (1)$$

where the wind force will be obtained from the HFFB test. The mean wind force ratio of the interfered principal building to that of the isolated principal building is used here to define the mean interference factor (hereafter referred to as mean *IF*). The dynamic response is the RMS of the dynamic response, σ_{M}, of the base moment (or displacement). According to the principle of the high frequency base force balance technique [23], σ_{M} can be easily computed by

$$\sigma_{\mathrm{M}} = \sigma_{M_s}\sqrt{1 + \frac{\pi}{4}\frac{1}{\zeta_0}\frac{\chi_0 S_{M_s}(\chi_0)}{\sigma^2_{M_s}}}, \quad (2)$$

where M_s is the base moment of the principal building model from the test; $\chi S_{M_s}(\chi)/\sigma^2_{M_s}$ is the dimensionless power spectrum density (PSD) of M_s. $\chi_0 (= f_0 D/V_{\mathrm{H}}$, V_{H} is the wind velocity at the top of the principal building) is the reduced fundamental frequency. It can be seen that σ_{M} is related to the value of the PSD at the reduced frequency, χ_0, or in other words, at the reduced velocity $V_{\mathrm{r}} (= V_{\mathrm{H}}/f_0 D = 1/\chi_0)$. For the computation of dynamic response, the main dynamic characteristics of the prototype of typical principal building are assumed to be: height of 240 m; breadth of 40 m; structural damping of $\zeta_0 = 2\%$ of critical damping; and natural frequency of $f_0 = 0.2$ Hz for both sway fundamental modes. Moreover, the reduced velocities adopted in the computation vary from 2 to 9, which cover a common range of wind velocity for most tall buildings [24].

In fact, the interference effects among three buildings are very complex and difficult to be expressed in a simple manner. In order to simplify the complexity of the problem and further formulate some clauses for building structural design codes, an envelope interference factor (*EIF*) is proposed here to describe the dynamic interference effects by maximizing the *IF*s in the reduced velocity ranges of $V_{\mathrm{r}} = 2$–9, i.e.

$$EIF = \max_{V_{\mathrm{r}}\in[2,9]} IF(V_{\mathrm{r}}), \quad (3)$$

where the reduced velocities higher than 9 rarely occur for practical structures and are therefore not considered.

Furthermore, regression analyses of the interference factors are made, and a new *IF* called regression *IF* (hereafter referred to as *RIF*) is proposed to describe the regression result of *IF* hereafter.

In Eq. (1), the wind pressure will be obtained in the wind pressure measurement test. The ratio of peak wind pressure coefficient of the interfered principal building to that of isolated principal building is adopted to express the wind pressure interference factor (*WP-IF* in short), where the peak pressure coefficient is given by

$$C_{\mathrm{p,peak}} = \left|\bar{C}_{\mathrm{p}}\right| + gC_{\mathrm{p,rms}}, \quad (4)$$

where $\bar{C}_{\mathrm{p}}$ is the mean wind pressure coefficient; g is the peak factor, taking 3.5 here; $C_{\mathrm{p,rms}}$ is the RMS wind pressure coefficient.

3 Mean interference factor

3.1 Typical mean *IF*

Statistical results for a thorough description of the mean interference effects for two- and three-building configurations in exposure category B are first shown in Fig. 3, where p represents the percentage of the positions of the corresponding interference factor over the whole test positions of the configurations. From this figure, one can see that the p is 35% when *IF* is about equal to 1.0 for the two-building configuration, but only about 13% for the three-building configuration. In general, for different levels of mean $IF \le 0.9$, the value of p of three-building configuration is greater than that of two-building configuration. These results indicate that the shielding effects of three-building configuration are more significant than two-building configuration.

The channeling effect was also found in the tests. The maximum mean *IF* was found to be 1.04 in the present test for the two-building configuration and 1.10 for the configuration of three equal size buildings. For the three-building configuration, the mean *IF* is about 1.1 for 2% of the complete set of interfering building arrangements. In fact, the channeling effect was also mentioned in ASCE 7-98.

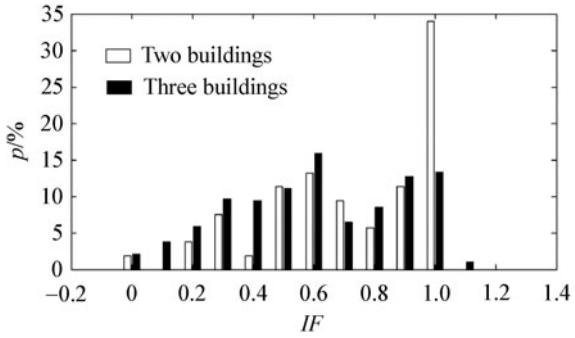

Fig. 3 Comparison of distribution of mean IF between the configurations of two and three identical buildings

3.2 Effect of breadth ratio of three-building configuration

The statistical properties for the interference effects of five groups of interfering buildings for the three-building configuration in exposure category B are shown in Fig. 4. From this figure, one can see that the most notable shielding region of $IF \leq 0.4$ increases quickly with the increase of B_r; while the regions of $0.5 \leq IF \leq 0.9$ remain unchanged relatively. But for the channeling effect, the variation of mean IF with B_r is contrary to the shielding situation. The increase of the building size could enhance the adverse static amplification on the principal building when the two interfering buildings are located at some critical locations. For the five types of breadth of interfering buildings, it was found that the critical positions for both two interfering buildings were about $(0, \pm 3.2b)$ in the present test grid region shown in Fig. 2, and the corresponding maximum interference factors for $B_r = 0.5$, 0.75, 1.0, 1.5 and 2.0 in exposure category B were 1.03, 1.05, 1.10, 1.15 and 1.20, respectively. This means that the two symmetrically located larger sized interfering buildings with $B_r = 2$ can increase 20% mean wind load on the middle principal building.

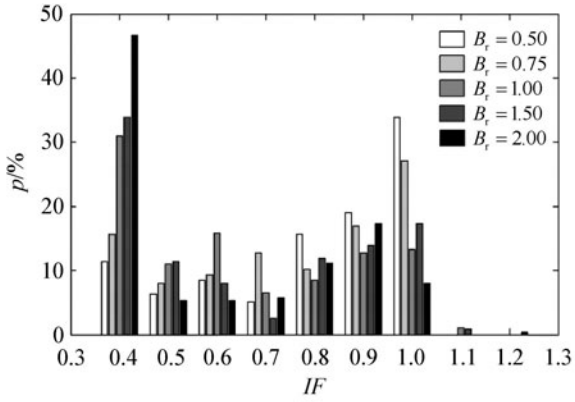

Fig. 4 Statistical results of mean IFs for different B_r's

The variations of mean RIF with varying B_r of the interfering buildings can be linearly regressed and some of the results are presented in Fig. 5, which shows that for most of the positions of the interfered buildings the mean RIF decreases with the increase of B_r. The regression results of mean IF for different breadth ratios can be fitted with linear formulas with correlation coefficient of about 0.99 [25].

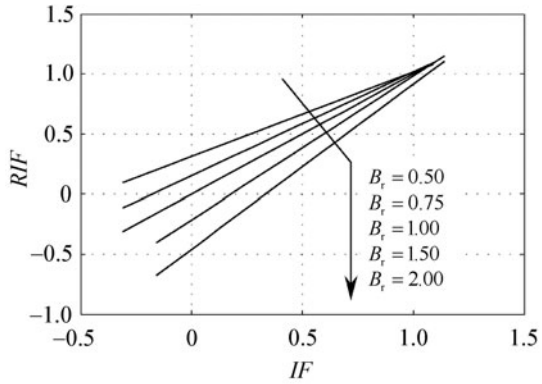

Fig. 5 Regression results of mean IFs for different B_r's

3.3 Effects of height ratio of three-building configuration

Figure 6 presents the statistical distributions of mean interference effects for the two interfering buildings with different height ratios in exposure category B. The results show that two lower interfering buildings of $H_r = 0.5$ produce insignificant interference effects, with most of the interference factors being within the range [0.9, 1.0] in exposure category B, also in exposure category D. Furthermore, it can be summarized from Fig.6 that the sensitive height of interfering buildings for the mean interference effects are in the range from $0.5h$ to $1.25h$, while the interference effects remain almost the same for higher interfering buildings. However, the higher interfering buildings may cause stronger channeling effects. The regression curves of the mean RIF for configurations with different height ratios in exposure category B are shown in Fig. 7, and the mean RIFs for different height ratios have been simply formulated in Ref. [16].

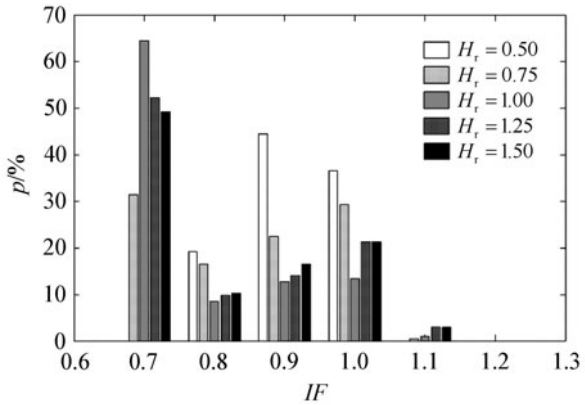

Fig. 6 Statistical results of mean IFs for different H_r's

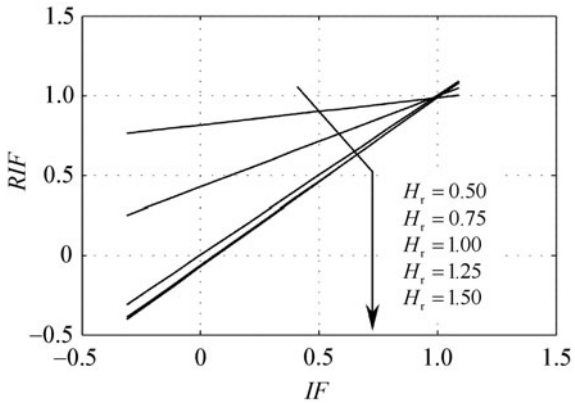

Fig. 7 Regression results of mean *IF* for different H_r's

Moreover, for the effect of the upstream terrains on the mean *IF* of the configuration of different H_r's, strong linear correlations exist in the mean *IF*s between the two upwind terrains for all the configurations of height ratio. The mean *IF* of any configuration of H_r in exposure category D can be simply predicted from the corresponding mean *IF* in exposure category B by

$$MIF_D = 0.078 + 0.982MIF_B. \quad (5)$$

4 Dynamic interference

4.1 Comparison between two buildings and three buildings

Statistical analysis for a thorough description of the dynamic interference effects in along- and across-wind directions was made and the results are shown in Fig. 8, where *p* represents the percentage of the positions of the corresponding *EIF* over the whole test positions of the configurations. From Fig. 8a, it can be seen that when $EIF \leq 2$, the values of *p* of the two-building configuration in along-wind direction are larger than those of the three-building configuration; but when $EIF > 2$, the situation is just opposite. For example, *p* is 15% when *EIF* is about equal to 2.5 for the three-building configuration, but only about 7.5% for the two-building configuration. And the *EIF*s can be still greater or equal to 3 for 10% of the complete set of interfering building arrangements. This obviously reveals that two interfering buildings can produce stronger interference effects than a single interfering building in the along-wind direction. But one can see that the interference effects in the across-wind direction arrangement caused by two interfering buildings are generally weaker than those by a single interfering building for most of the interfering building arrangements, as shown in Fig. 8b. In the figure, the *p* is 38.5% when *EIF* is about 1.0 for the three-building configuration, but only about 15.1% for the two-building configuration. Moreover, for different levels of $EIF = 1.5$, 2 and 2.5, the values of *p* of the two-building configuration are all greater than those of the three-building configuration. Even so, the *EIF* is found to be greater or equal to 3 for 1% of the whole sets of interfering building arrangements of the three-building configuration.

4.2 Effect of height ratio of three-building configuration

Results revealing the effects of the two interfering buildings with different heights on the dynamic *IF*s are presented here. There is an indication from the regression analysis that *EIF*s between different height ratios ($H_r = 0.5$, 0.75, 1.0, 1.25 and 1.5) still show linear correlations. Figure 9 presents the regression results of the *EIF*s for different height ratios in exposure category B. Generally, the dynamic *IF*s increase with the height of the interfering building, while the effects can be neglected for $H_r < 0.5$; and furthermore, the *EIF*s increase more rapidly with the increase of H_r in the along-wind direction than in the across-wind direction.

Based on a great quantity of computation, the regression relations of *EIF*s for different H_r's can be expressed by Eq. (6), for which the values of C_1 and C_2 are listed in Table 1.

$$RIF = C_1 + C_2EIF. \quad (6)$$

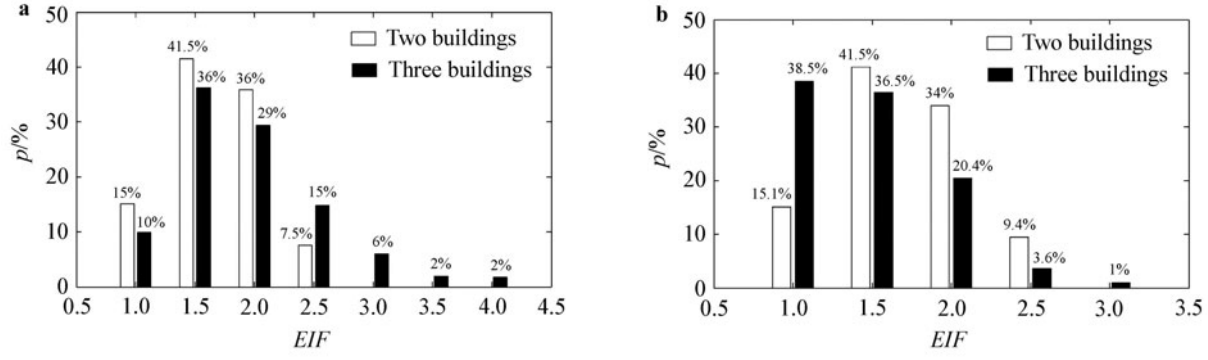

Fig. 8 Comparison of distribution of *EIF* between two-building and three-building configurations. **a** Al-W; **b** Ac-W

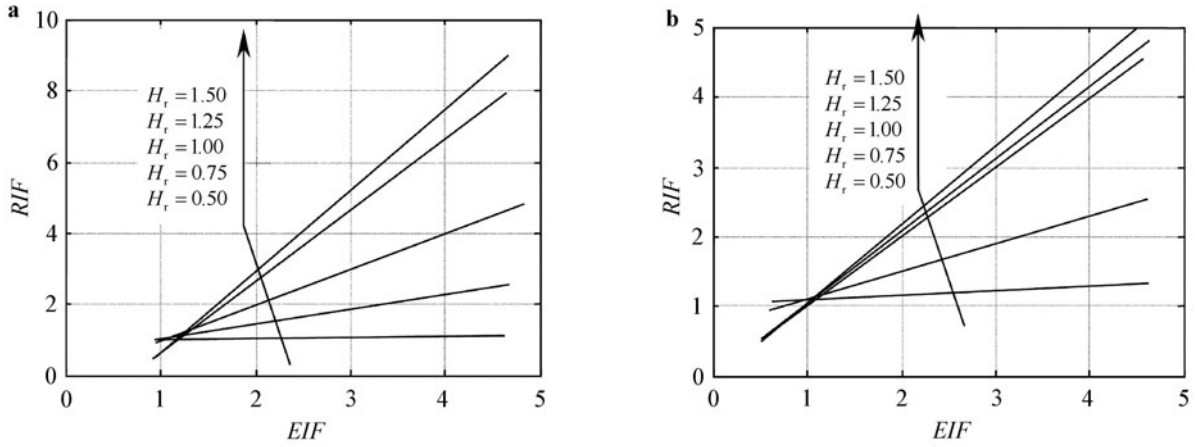

Fig. 9 Regression results of EIF for different H_r's. **a** Al-W; **b** Ac-W

Table 1 Values of C_1 and C_2 in Eq. (6)

H_r	0.50		0.75		1.00		1.25		1.50	
	C_1	C_2	C_1	C_2	C_1	C_2	C_1	C_2	C_1	C_2
Al-W	1.011	0.031	0.698	0.408	0	1	−1.317	1.988	−1.524	2.256
Ac-W	1.018	0.068	0.627	0.450	0	1	−0.028	1.038	−0.067	1.118

4.3 Effect of breadth ratio

It seems difficult to find satisfactory regression dynamic factors for breadth ratio as those for height ratio from the wind tunnel tests. Detailed discussions on this subject were made by the authors in Ref. [25] but will not be repeated here.

4.4 Effect of upstream terrain

Figure 10 illustrates variations of EIF for the three-building configurations with different height ratios in exposure category D versus the variations in exposure category B, where EIF_B and EIF_D are the EIF in exposure categories B and D, respectively. The relations between EIF_B and EIF_D in the along-wind direction can be expressed by linear formulas, while the relations between EIF_B and EIF_D in the across-wind direction for the height ratio of $H_r \geq 1$ are expressed by a second-order regression polynomial rather than a linear formula. Then, the relation of the EIFs between the two upstream terrains for all the height ratio configurations can be expressed by Eq. (7) for both the along-wind and the across-wind directions. The constants in Eq. (7), C_1, C_2 and C_3, are derived based on the test data and listed in Table 2, where Al-W means the along-wind direction; while Ac-W means the across-wind direction. Besides, $C_3 = 0$ for the cases of $H_r = 0.5$ and 0.75.

$$EIF_D = C_1 + C_2 EIF_B + C_3 (EIF_B)^2. \quad (7)$$

As for the variations of EIF for different B_r's in exposure categories D versus those in category B, regression results can be found in Ref. [16].

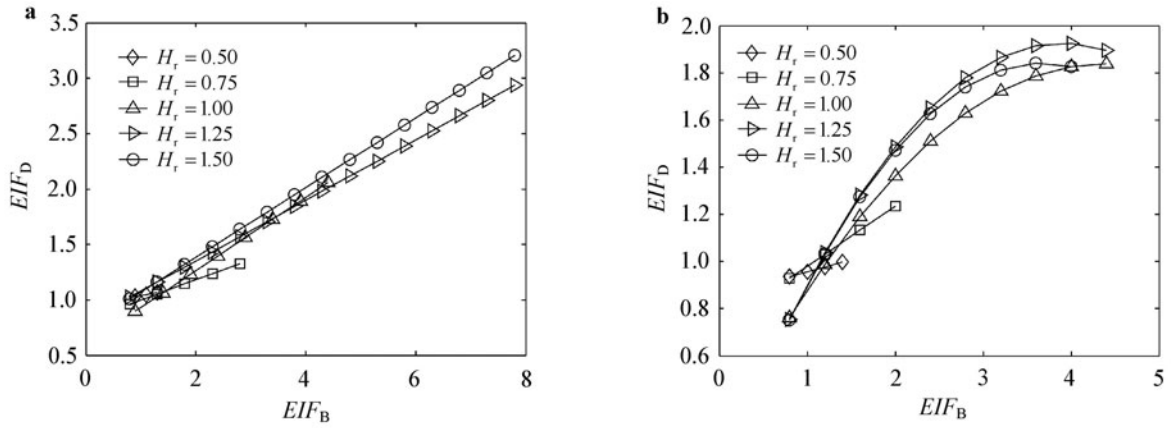

Fig. 10 Regression EIFs between different upwind terrains for different H_r's. **a** Al-W; **b** Ac-W

Table 2 Values of C_1, C_2 and C_3 in Eq. (7)

H_r	0.50		0.75		1.00			1.25			1.50		
	C_1	C_2	C_1	C_2	C_1	C_2	C_3	C_1	C_2	C_3	C_1	C_2	C_3
Al-W	0.946	0.093	0.819	0.181	0.599	0.332	0	0.806	0.273	0	0.757	0.314	0
Ac-W	0.853	0.103	0.725	0.255	0.227	0.736	−0.084	0.072	0.951	−0.238	0.059	0.970	−0.132

5 Peak wind pressure interference factor (*WP-IF*)

5.1 *WP-IF* of two-building configuration

Compared with the mean and dynamic *IF*s discussed above, the problem of *WP-IF* is much more complicated. Thus only *WP-IF*s at one selected typical point, i.e., Point P_1 indicated above, of the principal building interfered by one building are first presented. Figure 11 presents the *WP-IF* distributions when the interfered building is located in different positions for different wind conditions. From the figure it can be seen that for most of the interfering positions the *WP-IF*s are larger than unity, which means that peak wind pressure might be amplified by the surrounding buildings; and moreover the *WP-IF*s in higher turbulence condition are generally smaller than those in lower turbulence condition.

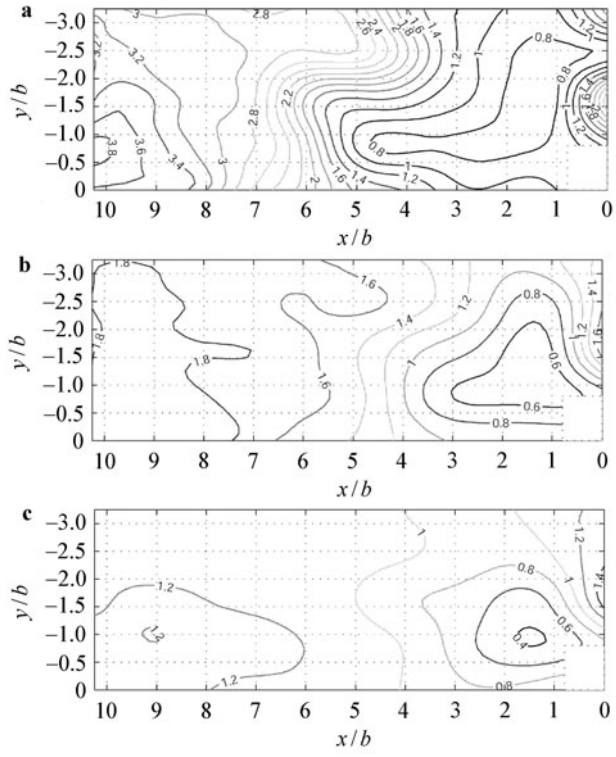

Fig. 11 WP-IF of two-building configuration. **a** Smooth flow; **b** Exposure category B; **c** Exposure category D

Figure 12 shows the PSDs of wind pressures at Point P_1 of the principal building for the interfered building located at the critical position $(10.1b, -0.8b)$ together with that of the isolated principal building in terrain category B. The comparison results indicate that the wind pressure energy at most of the key positions of the principal building will be amplified in almost all the frequency range due to interference.

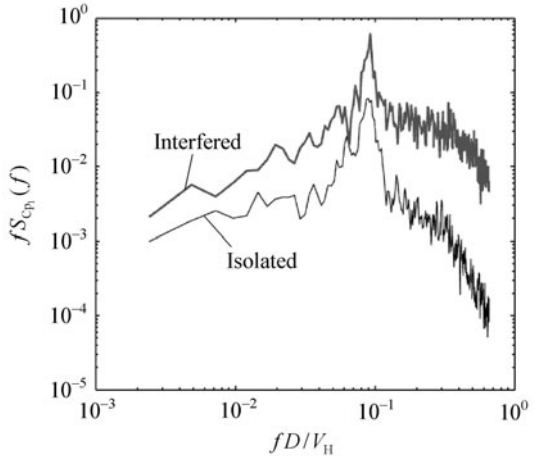

Fig. 12 PSDs of wind pressures at Point P_1 for interfered building and isolated building

5.2 *WP-IF* of three-building configuration

5.2.1 General distribution of WP-IF

Testing results reveal that the maximum *WP-IF*s of the three-building configuration are generally larger than those of the two-building configuration, which is similar to the situation for dynamic *IF*. Comparison of the maximum *WP-IF*s for typical conditions are shown in Table 3.

In fact, the *WP-IF* of three-building configuration is difficult to graphically expressed due to too many variables. To simplify the graphical expression of the results, one of the two interfering buildings is fixed at its critical position, while the position of the other interfering building can be varied. Through this approach, we can find distribution pattern of key *WP-IF*. Figure 13 shows one set of typical results. In this figure, when Model A is fixed at the position of $(6.1b, -0.8b)$, and furthermore Model B is located at $(1.1b, -2.4b)$, the maximum *WP-IF* is 2.2. Based on a great quantity of computation, the distribution critical of key *WP-IF* is summarized and shown in Fig. 14.

Table 3 Maximum peak wind *WP-IF*

	Terrain	Side by side	Arbitrary position
Two-buildings	Category B	1.73 $(0, -1.6b)$	1.93 $(10.1b, -0.8b)$
	Category D	1.50$(0, -1.6b)$	1.31$(9.1b, 0)$
Three-buildings	Category B	1.89 $(0, -3.2)(0, -1.6)$	2.19 $(1.1, -2.4)(6.1, -0.8)$
	Category D	1.71 $(0, -3.2)(0, -1.6)$	1.74 $(0, -1.6)(8.1, 1.6)$

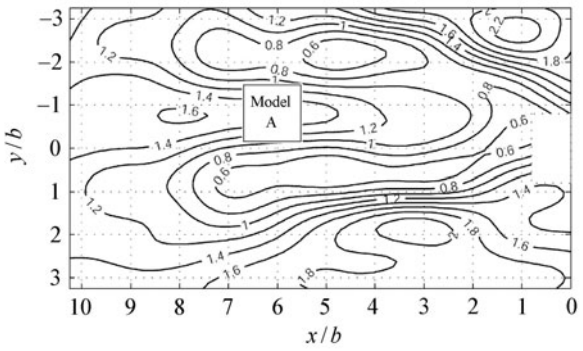

Fig. 13 *WP-IF* for Model A fixed at $(6.1b, -0.8b)$ and Model B at different position (Terrain B)

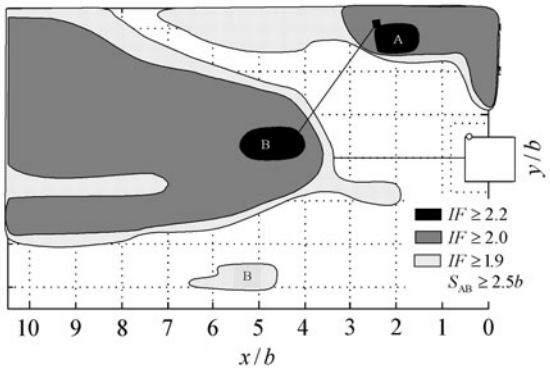

Fig. 14 Critical distributions of *WP-IF* at Point P_1 for three-building configuration (Terrain B)

5.2.2 *Effects of building parameters and terrain condition*

Statistical results of the *WP-IF*s at Point P_1 of the principal building for the basic three-building configuration, i.e., three identical buildings, in three categories of terrains, are presented in Fig. 15, where vertical coordinate p represents the percentage of the *WP-IF* over the whole test positions of the three-building configuration for the three categories of wind fields. From the figure, it can be seen that the *WP-IF*s in rougher terrain conditions are statistically smaller than those in smoother terrain conditions.

Similar to the mean and dynamic *IF*s, regression analysis method is also tried for the *WP-IF*. Basic variation patterns of the *WP-IF* at Point P_1 for different breadth ratios and height ratios are graphically summarized in Figs. 16 and 17, respectively; and the corresponding formulas have been derived in Ref. [25].

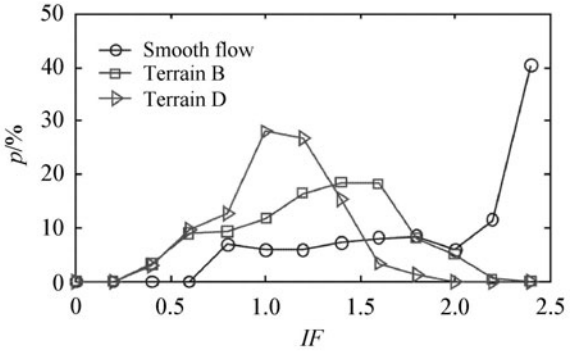

Fig. 15 Statistical results of *WP-IF*s for three building configurations

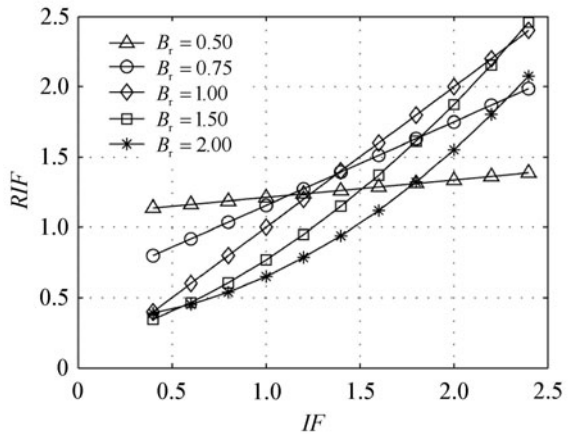

Fig. 16 *WP-RIF*s for different B_r's

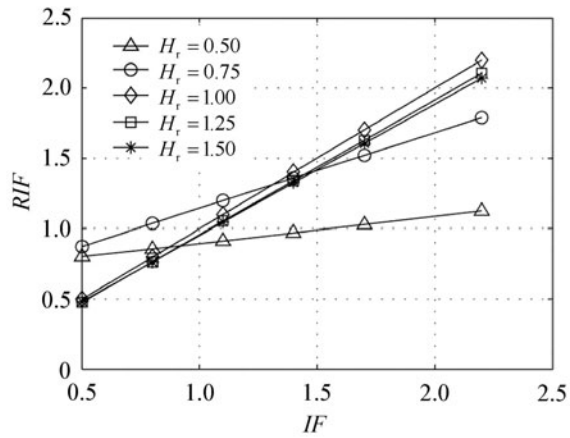

Fig. 17 *WP-RIF*s for different H_r*'s*

6 Concluding remarks

In this paper, mean and dynamic interference effects as well as peak wind pressure interference effects for two and three tall buildings, especially the three-building configuration, are studied based on a series of wind tunnel tests on typical tall building models. Effects of relevant parameters on the interference factors are investigated in-depth and major regression results of the interference factors are presented. Some of the main results can be summarized as follows:

(1) Two interfering buildings can generally produce stronger shielding effects on the mean force acting on the principal building than a single interfering building. Moreover, two interfering buildings can produce stronger along-wind dynamic interference effects (amplification effects) than a single interfering building, but the dynamic interference effects in the across-wind direction caused by two interfering buildings seem to be somewhat weaker than those by a single interfering building for most of usual arrangements of interfering buildings.

(2) It is highlighted in this study that two upstream buildings can bring about more complicated dynamic effects on the principal building than a single upstream building does. An effective method is proposed to introduce an envelope interference factor (EIF) and use its critical distribution to describe the interference effects among three tall buildings.

(3) Higher and wider interfering building(s) can produce stronger shielding effects on the mean wind force acting on the principal building; and similarly higher and wider interfering building(s) can produce stronger amplification effect on the dynamic forces on the principal building whilst the effect of the interfering building with Hr smaller than 0.5 can be neglected.

(4) Significant correlations exist in the mean and dynamic interference factors for different configurations of height ratios and upwind terrains. Regression equations reflecting the inherent complex relationships are proposed to simplify the expressions of interference effects. But it seems difficult to find satisfactory regression dynamic factors for breadth ratio as those for height ratio from the wind tunnel tests.

(5) The maximum *WP-IF*s of the three-building configuration are generally larger than those of the two-building configuration, which is similar to the situation for dynamic *IF*. The *WP-IF*s in rougher terrain conditions are statistically smaller than those in smoother terrain conditions.

References

1 Saunders, J.W., Melbourne, W.H.: Buffeting effects of upwind buildings. In: Proceedings of the 5th International Conference on Wind Engineering, Fort Collins, Pergamon Press, Oxford, 593–605 (1980)

2 Kareem, A.: Effect of aerodynamic interference on the dynamic response of prismatic structures. J. Wind Eng. Ind. Aerodyn. **25**(3), 365–372 (1987) DOI 10.1016/0167-6105(87)90028-6

3 Kwok, K.C.S.: Interference effects on tall buildings, Recent advances in wind engineering. In: Proceedings of the 2nd Asia-Pacific Symp. Wind Engng, Beijing, China, **1**, 446–453 (1989)

4 Kwok, K.C.S.: Aerodynamics of the tall buildings: A state-of-the-art in wind engineering. In: Proceedings of the 9th International Conference on Wind Engineering, New Delhi, India, 180–204 (1995)

5 Khanduri, A.C., Stathopoulos, T., Bédard, C.: Wind-induced interference effects on buildings—A review of the state-of-the-art. Eng. Struct. **20**(7), 617–630 (1998) DOI 10.1016/S0141-0296(97)00066-7

6 Bailey, P.A., Kwok, K.C.S.: Interference excitation of twin tall buildings. J. Wind Eng. Ind. Aerodyn. **21**(3), 323–338 (1985) DOI 10.1016/0167-6105(85)90043-1

7 Taniike, Y., Inaoka, H.: Aeroelastic behaviour of a tall building in wakes. J. Wind Eng. Ind. Aerodyn. **28**(1-3), 317–327 (1988) DOI 10.1016/0167-6105(88)90128-6

8 Taniike, Y.: Turbulence effect on mutual interference of buildings. J. Eng. Mech.-ASCE **117**(3), 443–456 (1991) DOI 10.1061/(ASCE)0733-9399(1991)117:3(443)

9 Taniike, Y.: Interference mechanism for enhanced wind forces on neighbouring tall buildings. J. Wind Eng. Ind. Aerodyn. **42**(1-3), 1073–1083 (1992) DOI 10.1016/0167-6105(92)90114-P

10 English, E.C.: Shielding factors for paired rectangular prisms: An analysis of along-wind mean response data from several sources. In: Proceedings of 7th U.S. National Conference on wind Engineering. University of California, Los Angeles, CA, 193–201 (1993)

11 English, E.C.: The interference index and its prediction using a neural network analysis of wind-tunnel data. J. Wind Eng. Ind. Aerodyn. **83**(1-3), 567–575 (1999) DOI 10.1016/S0167-6105(99)00102-6

12 Gu, M., Xie, Z.N., Huang, P.: Along-wind dynamic interference effects of tall buildings. Adv. Struct. Eng. **8**(6), 623–635 (2005) DOI 10.1260/136943305776318400

13 Huang, P., Gu, M.: Experimental study of wind-induced dynamic interference effects between two tall buildings. Wind Struct. **8**(3), 147–161 (2005)

14 Xie, Z.N., Gu, M.: A correlation-based analysis on wind-induced interference effects between two tall buildings. Wind Struct. **8**(3), 163–178 (2005)

15 Xie, Z.N., Gu, M.: Mean interference effects among tall buildings. Eng. Struct. **26**(9), 1173–1183 (2004) DOI 10.1016/j.engstruct.2004.03.007

16 Xie, Z.N., Gu, M.: Simplified formulas for evaluation of wind-induced interference effects among three tall buildings. J. Wind Eng. Ind. Aerodyn. **95**(1), 31–52 (2007) DOI 10.1016/j.jweia.2006.05.003

17 Xie, Z.N., Gu, M.: Across-wind dynamic response of high-rise building under wind action with interference effects from one and two tall buildings. Struct. Des. Tall Spec. Struct. **18**(1), 37–57 (2009) DOI 10.1002/tal.393

18 Chen, S.Q., Gu, M., Huang, Z.P.: Numerical computation of the flow around two square cylinders arranged side-by-side.

Appl. Math. Mech. **21**(2), 147–164 (2000)
19 Zhang, A.S., Gu, M.: Wind tunnel tests and numerical simulations of wind pressures on buildings in staggered arrangement. J. Wind Eng. Ind. Aerodyn. **96**(10-11), 2067–2079 (2008) DOI 10.1016/j.jweia.2008.02.013
20 Jozwiak, R., Kacprzyk, J., Zuranski, J.A.: Wind tunnel investigations if interference effects on pressure distribution on a building. J. Wind Eng. Ind. Aerodyn. **57**(2-3), 159–166 (1995) DOI 10.1016/0167-6105(95)00004-B
21 Cheng C.M., Wang, J.: Wind tunnel database for an intermediate wind resistance design of tall buildings. In: Proc. of the First International Symposium on Wind Effects on Buildings and Urban Environment, Tokyo, Japan (2004)
22 Chinese Load Code for Design of Building Structures (GB50009-2001). Architectural Industry Press of China, Beijing (2002)
23 Tschanz, T., Davenport, A.G.: The base balance technique for the determination of dynamic wind loads. J. Wind Eng. Ind. Aerodyn. **13**(1-3), 429–439 (1983) DOI 10.1016/0167-6105(83)90162-9
24 Gu, M., Quan, Y.: Across-wind loads of typical tall buildings. J. Wind Eng. Ind. Aerodyn., **92**(13), 1147–1165 (2004) DOI 10.1016/j.jweia.2004.06.004
25 Xie, Z.N.: Study on wind induced interference effects of typical tall buildings. [Ph.D. Dissertation], Tongji University, China (2004)